Eur. Phys. J. B **33**, 297–310 (2003)
DOI: 10.1140/epjb/e2003-00170-y

THE EUROPEAN PHYSICAL JOURNAL B

Modelling of magnetic effects in near-field optics*

U. Schröter[a]

Fachbereich Physik, Universität Konstanz, Universitätsstrasse 10, 78457 Konstanz, Germany

Received 15 December 2002
Published online 20 June 2003 –

Abstract. Green's dyadic technique represents a powerful tool for calculations in electrodynamics, especially in modelling optical properties of nanoscopic objects. The method does not only provide field distributions, but also maps of susceptibilities and densities of states. Whereas the formalism is well established for dielectrics and electric fields, I present here a straight forward extension to tensors of both electric and magnetic type as well as mixed ones and furthermore to the situation where objects with dielectric and magnetic permeabilities are present together. As examples, characteristic field patterns are compared for elementary dielectric and magnetic perturbations. Green's tensors calculated for a coral structure reveal that mixed susceptibilities can exhibit other symmetries than pure electric or magnetic ones. Maps of all tensor components can thus give essential clues to the interpretation of near-field images.

PACS. 41.20.-q Applied classical electromagnetism – 78.20.Bh Theory, models, and numerical simulation – 02.60.Cb Numerical simulation; solution of equations

1 Introduction

Nanofabrication techniques today offer the possibility of tayloring optical properties on a microscopic scale, to achieve highly localized field enhancements for example [1–3]. Near-field scanning even allows mapping of optical quantities in the vicinity of nanoscopic objects. The influence of the probe tip and its shape on the detection process, however, is not at all obvious. This and the fact that studies of a great variety of objects with quite arbitrary shapes would be desirable makes numerical modelling an important tool in near-field optics. Green's dyadic technique [4–7] provides a direct space integration method to solve Maxwell's equations. Although it has successfully been applied to extended geometries like multilayer structures with translational symmetry in one or two dimensions [8–11], it is best suited for problems with nanoscopic objects respresenting a spatially limited perturbation in an otherwise homogeneous background, and this is the situation for which the form of the theory is presented here.

A pragmatic interpretation of near-field images consists in regarding the influence of the tip as part of the measurement process and trying to identify the optical signal with a physical quantity as it would be without the tip present. Once a near-field scanning optical microscopy (NSOM) setup has been characterized in this way with the help of test samples, measurements of others then yield pure sample properties instead of information about the sample-tip system only. Excellent agreement between experimental results and calculations has repeatedly shown that a photon scanning tunneling microscope (PSTM) normally maps the electric field, which of course depends on the direction of incident waves. Examples include dielectric and metallic protrusions [12–14], waveguides [15,16], chains of metal particles exhibiting near-field squeezing [17] and metallic stripes suited for surface plasmon propagation [18]. NSOM in illumination mode with forbidden light detection, however, images the local density of states of the electric field, a property determined by the material distribution alone [19] as demonstrated by Chicanne *et al.* [20] on an optical coral structure in analogy to quantum corals for electronic densities of states [21]. The local density of states can be viewed as the response to an ideal dipole source at the respective point. Returning to PSTM (NSOM in collection mode), recent experiments by Devaux *et al.* [22,23] surprisingly showed that specially coated tips can map the local magnetic field. These observations have clearly brought to the fore that measurement can distinguish between the electric and the magnetic field [24]. The NSOM signal was identified to the magnetic field with the help of modelling by Green's dyadic technique [25]; sources and objects for this case were still of dielectric type, though.

The sensitivity of the tips to the optical magnetic field is made possible by a gold coating whose thickness has to be adapted to the wavelength of the light used. Metal cylinders or rings of dimensions of optical wavelengths can sustain surface plasmon modes [26] with magnetic dipole moment comparable or even exceeding the electric dipole moment for frequencies in the visible [27]. Now, one could think of taking structures with such magnetic

* Files "maths.ps" and "tensors.ps" are only available in electronic form at `http://www.edpsciences.org`

[a] e-mail: `Ursula.Schroeter@uni-konstanz.de`

permeability not only as detectors, but as objects under investigation themselves; sources of magnetic dipole type should also be considered. Thus also modelling fully including magnetic effects is required.

To make the presentation somewhat self-consistent, the Green's tensor method as used for dielectric perturbations and electric fields is briefly reviewed in Section 2. Magnetic and mixed suceptibilities are then developed in Section 3 still staying with dielectric objects. The situation with pure magnetic permeabilities is fully analogous and shortly discussed in Section 4. With these preparations Green's tensors for the generalized situation with both dielectric and magnetic permeabilities are then constructed in Section 5. Whereas the densities of states can be directly read off from the tensors, Section 6 describes how to calculate the field distributions. Some examples are finally given in Section 7.

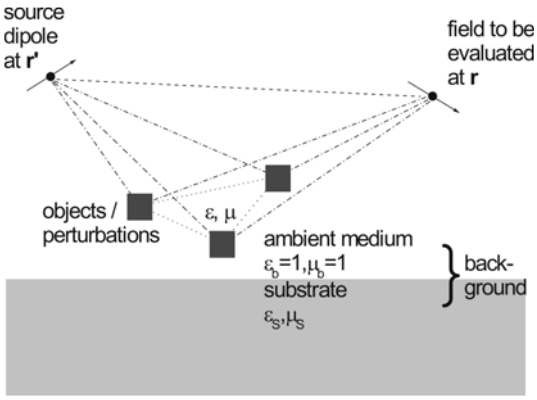

Fig. 1. A given material distribution is divided into a background and some perturbation objects. The field at $\mathbf{r}$ caused by some dipole source at $\mathbf{r}'$ consists of the directly propagated part and a contribution *via* the interaction with the objects.

2 Green's dyadic technique

In near-field optics experiments we often deal with monochromatic light, but as any wave packet can be decomposed into a superposition of plane waves, it is without loss of generality that we assume monochromatic electric and magnetic fields with time dependence $\mathrm{e}^{-\mathrm{i}\omega t}$. Maxwell's equations then read in cgs units:

$$\nabla \cdot \mathbf{E}(\mathbf{r}) = -4\pi \nabla \cdot \mathbf{P}(\mathbf{r}) \tag{2.1}$$

$$\nabla \cdot \mathbf{H}(\mathbf{r}) = -4\pi \nabla \cdot \mathbf{M}(\mathbf{r}) \tag{2.2}$$

$$\nabla \wedge \mathbf{E}(\mathbf{r}) = \mathrm{i}k_0 \mathbf{H}(\mathbf{r}) + 4\pi \mathrm{i}k_0 \mathbf{M}(\mathbf{r}) \tag{2.3}$$

$$\nabla \wedge \mathbf{H}(\mathbf{r}) = -\mathrm{i}k_0 \mathbf{E}(\mathbf{r}) - 4\pi \mathrm{i}k_0 \mathbf{P}(\mathbf{r}) \tag{2.4}$$

with $k_0 = \omega/c$. Without external charges, currents or magnetizations the polarization $\mathbf{P}$ and the magnetization $\mathbf{M}$ are related to the fields by

$$\mathbf{P}(\mathbf{r}) = \frac{\varepsilon(\mathbf{r}) - 1}{4\pi} \mathbf{E}(\mathbf{r}) \quad \text{and} \quad \mathbf{M}(\mathbf{r}) = \frac{\mu(\mathbf{r}) - 1}{4\pi} \mathbf{H}(\mathbf{r}) \tag{2.5}$$

$\varepsilon(\mathbf{r})$ and $\mu(\mathbf{r})$ may in general be tensors, that is direction depending. Green's dyadic technique as presented here can be applied to solve Maxwell's equations if only in a finite region the permeabilities $\varepsilon(\mathbf{r})$ and $\mu(\mathbf{r})$ differ from background values which for simplicity are both assumed to be 1, although other constant background values ε_b and μ_b would not at all complicate the procedure. Throughout this section and the next we further assume $\mu(\mathbf{r}) = 1$ everywhere. In this case (2.3) and (2.4) can be combined to give the wave equation

$$-\nabla \wedge \nabla \wedge \mathbf{E}(\mathbf{r}) + k_0^2 \mathbf{E}(\mathbf{r}) = -4\pi k_0^2 \frac{\varepsilon(\mathbf{r}) - 1}{4\pi} \mathbf{E}(\mathbf{r}) \tag{2.6}$$

where we have splitted the term proportional to $\mathbf{E}$ in a homogeneous part on the left and an ε-depending part on the right side. The latter is only present in a region A where the dielectric function differs from the background, that is where $\varepsilon(\mathbf{r}) \neq 1$.

The key concept of Green's dyadic technique is the tensor G^0 satisfying

$$-\nabla \wedge \nabla \wedge G^0(\mathbf{r}, \mathbf{r}') + k_0^2 \, G^0(\mathbf{r}, \mathbf{r}') = -4\pi k_0^2 \, \mathbf{1} \, \delta(\mathbf{r} - \mathbf{r}'). \tag{2.7}$$

Derivatives are with respect to $\mathbf{r}$ and $\mathbf{1}$ is the unit matrix. G^0 is analytically known and with the help of the scalar function

$$g^0(\mathbf{r}, \mathbf{r}') = \frac{\mathrm{e}^{\mathrm{i}k_0|\mathbf{r}-\mathbf{r}'|}}{|\mathbf{r} - \mathbf{r}'|} \tag{2.8}$$

can be expressed as

$$G^0(\mathbf{r}, \mathbf{r}') = (\mathbf{1}k_0^2 + \nabla\nabla) g^0(\mathbf{r}, \mathbf{r}'). \tag{2.9}$$

The meaning of G^0 is the following: An electric dipole $\mathbf{p}$ placed at $\mathbf{r}'$ has the electric field $G^0(\mathbf{r}, \mathbf{r}')\mathbf{p}$ at $\mathbf{r}$. The influence of a planar surface (see Fig. 1) can be included, which is mostly done in the so-called electrostatic approximation [25]. G^0 is then replaced by

$$G^h(\mathbf{r}, \mathbf{r}') = G^0(\mathbf{r}, \mathbf{r}') + G^S(\mathbf{r}, \mathbf{r}') \tag{2.10}$$

for which (2.7) remains valid (see Appendix A). Regarding the right side of (2.6) as a perturbation $-4\pi k_0^2 \mathbf{Q}(\mathbf{r})$ a solution of this wave equation is constructed by

$$\begin{aligned} \mathbf{E}(\mathbf{r}) &= \mathbf{E}^0(\mathbf{r}) + \int_A G^h(\mathbf{r}, \mathbf{r}') \mathbf{Q}(\mathbf{r}') \mathrm{d}\mathbf{r}' \\ &= \mathbf{E}^0(\mathbf{r}) + \int_A G^h(\mathbf{r}, \mathbf{r}') \chi(\mathbf{r}') \mathbf{E}(\mathbf{r}') \mathrm{d}\mathbf{r}'. \end{aligned} \tag{2.11}$$

The integral is over region A where $\chi(\mathbf{r}) = \frac{\varepsilon(\mathbf{r})-1}{4\pi}$ is not vanishing, and $\mathbf{E}^0(\mathbf{r})$ is a solution of the homogeneous wave equation

$$-\nabla \wedge \nabla \wedge \mathbf{E}^0(\mathbf{r}) + k_0^2 \, \mathbf{E}^0(\mathbf{r}) = 0. \tag{2.12}$$

As $\mathbf{Q}(\mathbf{r}) = \chi(\mathbf{r})\mathbf{E}(\mathbf{r})$ depends on $\mathbf{E}(\mathbf{r})$ itself, (2.11) is an integral equation, the implicit Lippmann-Schwinger

equation, for $\mathbf{E}(\mathbf{r})$. If $\varepsilon(\mathbf{r})$ only differs from 1 (or its background value) in a limited region A and we discretize this region into a finite number of cells $1,\ldots,N$ at locations $\mathbf{r}_1,\ldots,\mathbf{r}_N$, equation (2.11) becomes

$$\mathbf{E}(\mathbf{r}_n) = \mathbf{E}^0(\mathbf{r}_n) + \sum_{n'=1}^{N} G^h(\mathbf{r}_n,\mathbf{r}_{n'})\chi(\mathbf{r}_{n'})\mathbf{E}(\mathbf{r}_{n'})\triangle v \quad (2.13)$$

where $\triangle v$ is the volume of one cell. E^0 is the field of the incident wave as it would be without perturbing objects, that is in the homogeneous medium or for the background with a surface.

This now is a system of linear equations on $\mathbf{E}(\mathbf{r}_1),\ldots,\mathbf{E}(\mathbf{r}_N)$, which can be solved by a matrix inversion. In practice build $3N$-vectors E_A and E_A^0 which contain all the components of $\mathbf{E}(\mathbf{r}_1),\ldots,\mathbf{E}(\mathbf{r}_N)$ resp. $\mathbf{E}^0(\mathbf{r}_1),\ldots,\mathbf{E}^0(\mathbf{r}_N)$, a $3N\times 3N$-matrix G^h of all 3×3-blocks $G^h(\mathbf{r}_n,\mathbf{r}_{n'})$ and a $3N\times 3N$-matrix V with just the 3×3-tensors $\chi(\mathbf{r}_n)$ as diagonal blocks. The factor $\triangle v$ is also included in V. The last equation then reads

$$E_A = E_A^0 + G^h\ V\ E_A \quad (2.14)$$

and solved for E_A

$$E_A = (\mathbf{1} - G^h\ V)^{-1}\ E_A^0. \quad (2.15)$$

Once the electric field is known inside the perturbation A, it can be calculated everywhere. Outside the perturbation (region B) we get

$$E_B = E_B^0 + G^h\ V\ (\mathbf{1} - G^h V)^{-1}\ E_A^0 \quad (2.16)$$

or

$$\mathbf{E}_B(\mathbf{r}) = \mathbf{E}_B^0(\mathbf{r}) + \sum_{n=1}^{N}\sum_{n'=1}^{N} G^h(\mathbf{r},\mathbf{r}_n)V(\mathbf{r}_n) \times (\mathbf{1} - G^h V)^{-1}(\mathbf{r}_n,\mathbf{r}_{n'})\mathbf{E}_A^0(\mathbf{r}_{n'}). \quad (2.17)$$

We could solve for the electric field at several positions in region B and gather these values in a vector E_B. However, as (2.16) is no implicit equation to solve like (2.14), it suffices to calculate the field at one position at a time. If we do not take the big $3N\times 3N$ matrices like in (2.16), but 3×3 tensors, the matrix multiplications become summations over all positions in the perturbation region A, of course. Beware that in (2.17) the two coordinates are written outside the inverted tensor $(\mathbf{1}-G^hV)$. That means you first have to invert the big $3N\times 3N$ matrix and then take the 3×3 block that corresponds to the coordinate pair $(\mathbf{r}_n,\mathbf{r}_{n'})$.

From (2.16) we can read off the tensor G that leads from the initial field $\mathbf{E}^0(\mathbf{r})$, the field of a source or an incident wave, to the resulting field $\mathbf{E}(\mathbf{r})$.

$$\mathbf{E}(\mathbf{r}) = \mathbf{E}^0(\mathbf{r}) + \int_A G(\mathbf{r},\mathbf{r}')\chi(\mathbf{r}')\mathbf{E}^0(\mathbf{r}')\mathrm{d}\mathbf{r}' \quad (2.18)$$

with

$$G = G^h + G^h\ V\ (\mathbf{1} - G^h V)^{-1}\ G^h. \quad (2.19)$$

In practice the integration over region A always becomes a summation over a finite number of perturbation cells like in (2.13) or (2.17), which is implicitly understood for all tensor contractions resp. written as multiplication of big matrices in equations in the form of (2.14)-(2.16) or (2.19). To see how (2.19) is inferred from (2.16) and for further deductions to come it is useful to develop $(\mathbf{1} - G^hV)^{-1}$ into a series [6].

$$\begin{aligned}(\mathbf{1} - G^hV)^{-1} &= \mathbf{1} + G^hV + G^hVG^hV + \ldots \\ &= \mathbf{1} + G^hV(\mathbf{1} - G^hV)^{-1}. \end{aligned} \quad (2.20)$$

G is the solution to the so-called Dyson equation [28]

$$G = G^h\ +\ G^h\ V\ G \quad (2.21)$$

and in analogy to (2.7) fulfills [6]

$$-\nabla\wedge\nabla\wedge G(\mathbf{r},\mathbf{r}') + k_0^2(1+4\pi\chi(\mathbf{r}))\ G(\mathbf{r},\mathbf{r}') = -4\pi k_0^2\ \mathbf{1}\ \delta(\mathbf{r}-\mathbf{r}'). \quad (2.22)$$

This G, which will be denoted G_ε^{EE} from now on, is the electric-electric susceptibility for a given configuration of dielectric objects. That is, for objects with only ε (no μ) as sketched in Figure 1, $G_\varepsilon^{EE}(\mathbf{r},\mathbf{r}')\mathbf{p}$ is the electric field that will result at $\mathbf{r}$ if an electric point dipole $\mathbf{p}$ is placed at $\mathbf{r}'$.

Once the electric field is known in the perturbation region A, we can also calculate the magnetic field everywhere outside the perturbations in the ambient medium [22,23,25,29].

$$\mathbf{H}(\mathbf{r}) = \mathbf{H}^0(\mathbf{r}) - \mathrm{i}k_0\int_A Q^0(\mathbf{r},\mathbf{r}')\chi(\mathbf{r}')\mathbf{E}(\mathbf{r}')\mathrm{d}\mathbf{r}' \quad (2.23)$$

$\mathbf{H}^0(\mathbf{r})$ is the initial field and a solution of

$$-\nabla\wedge\nabla\wedge\mathbf{H}^0(\mathbf{r}) + k_0^2\ \mathbf{H}^0(\mathbf{r}) = 0 \quad (2.24)$$

$$Q^0 = \begin{pmatrix} 0 & -\frac{\partial g^0}{\partial z} & \frac{\partial g^0}{\partial y} \\ \frac{\partial g^0}{\partial z} & 0 & -\frac{\partial g^0}{\partial x} \\ -\frac{\partial g^0}{\partial y} & \frac{\partial g^0}{\partial x} & 0 \end{pmatrix} \quad (2.25)$$

for a homogeneous background. In the electrostatic approximation Q^0 is not modified by the presence of a surface. Explicit expressions for G^0, G^S and Q^0 can be found in references [6,25,29] and in an additional file to this article. $-\mathrm{i}k_0Q^0(\mathbf{r},\mathbf{r}')\mathbf{p}$ simply is the magnetic field at $\mathbf{r}$ produced by an electric point dipole $\mathbf{p}$ at $\mathbf{r}'$. In (2.23) the magnetic field is inferred from the electric field and this equation is only valid if the perturbations are dielectric, that is, if the electric permeability ε in region A differs from 1 (its background value) but the magnetic permeability μ does not.

3 Magnetic and mixed susceptibilities

G_ε^{EE} is the electric-electric susceptibility, that is, $G_\varepsilon^{EE}(\mathbf{r},\mathbf{r}')\mathbf{p}$ is the resulting electric field at $\mathbf{r}$ due to an

electric point dipole at $\mathbf{r}'$ with the influence of the objects present included. Analogously we would also like tensors giving the magnetic field caused by an electric point dipole, and the electric and magnetic fields due to a magnetic point dipole, that is magnetic-electric, electric-magnetic and magnetic-magnetic susceptibility tensors.

If the objects are purely dielectric, not magnetic, all that has to be evaluated self-consistently is the electric field inside the objects. All other propagators are known. I therefore compose the four susceptibility tensors in this case as follows:

$$G_\varepsilon^{EE} = G_E^h + G_E^h V(\mathbf{1} - G_E^h V)^{-1} G_E^h \tag{3.1}$$

$$G_\varepsilon^{HE} = -\mathrm{i}k_0 Q_{HE}^0 - \mathrm{i}k_0 Q_{HE}^0 V(\mathbf{1} - G_E^h V)^{-1} G_E^h \tag{3.2}$$

$$G_\varepsilon^{EH} = \mathrm{i}k_0 Q_{EH}^0 + \mathrm{i}k_0 G_E^h V(\mathbf{1} - G_E^h V)^{-1} Q_{EH}^0 \tag{3.3}$$

$$G_\varepsilon^{HH} = G_H^h + k_0^2 Q_{HE}^0 V(\mathbf{1} - G_E^h V)^{-1} Q_{EH}^0. \tag{3.4}$$

Here I now denote the background propagator G^h for the electric field by G_E^h, as depending on whether a substrate surface is included in the background or not, the one for the magnetic field G_H^h may be different. In the same way, the tensor Q^0 evaluating the magnetic field due to an electric point dipole is indexed Q_{HE}^0, and Q_{EH}^0 is the tensor giving the electric field caused by a magnetic dipole (see Appendix A). G_E^h, G_H^h, $-\mathrm{i}k_0 Q_{HE}^0$ and $\mathrm{i}k_0 Q_{EH}^0$ for a homogeneous medium are just the dipole field formula [30] written in a matrix form to cover all possible directions of $\mathbf{p}$. If $\varepsilon_b = 1$ and $\mu_b = 1$ for the background medium where the fields are to be evaluated, and if the electrostatic approximation is taken for the influence of a substrate surface, only G_E^h gets a correction G^S to G^0. G_H^h is approximated as G^0, and Q_{HE}^0 and Q_{EH}^0 are equal to Q^0 from (2.25).

G_ε^{EE} has already been explained and G_ε^{HE} can be seen from (2.23) if the expression for the electric field from (2.15) is inserted. For completeness I will nevertheless explain the construction of all four tensors here. If the source at $\mathbf{r}'$ in Figure 1 is an electric point dipole $\mathbf{p}$, its electric field is directly propagated to $\mathbf{r}$ by G_E^h; this is the first term in (3.1). The second term is the contribution from the interaction with the objects. The initial field in the perturbation cells is the one propagated from the dipole to the objects also by G_E^h, the last factor in the second term. Then the self-consistent solution of the Lippmann-Schwinger equation (2.14) gives the resulting field $(\mathbf{1} - G_E^h V)^{-1} G_E^h \mathbf{p}$ inside the objects. The perturbations now themselves act as electric dipoles. The contribution of each cell on top of that of the background medium is proportional to its susceptibility χ contained in V in front of the parenthesis in (3.1) and it is propagated from the object to $\mathbf{r}$ by G_E^h.

In G_ε^{HE} the first term $-\mathrm{i}k_0 Q_{HE}^0$ is the magnetic field of an electric dipole at $\mathbf{r}'$ propagated directly to $\mathbf{r}$. As the perturbations are dielectric, they are excited by an electric field, propagated from the dipole at $\mathbf{r}'$ to the objects by G_E^h as before. To change from the initial to the resulting field at the locations of the objects, again $(\mathbf{1} - G_E^h V)^{-1}$ is put in front of that. The excess of the dipole strengths of the perturbation cells over that of the background medium is accounted for by V. Like the source dipole at $\mathbf{r}'$, the object cells represent electric dipoles, so their magnetic field is propagated to $\mathbf{r}$ by $-\mathrm{i}k_0 Q_{HE}^0$.

Let us now suppose that the source at $\mathbf{r}'$ is a magnetic point dipole $\mathbf{m}$. To get its electric field somewhere, the propagator to choose is $\mathrm{i}k_0 Q_{EH}^0$. So $\mathrm{i}k_0 Q_{EH}^0$ is the first term as well as the last factor in the second term in (3.3). Again, given the initial electric field in the perturbations, $(\mathbf{1} - G_E^h V)^{-1}$ turns it into the resulting electric field, that add a contribution $G_E^h V$ times themselves to the electric field somewhere else at $\mathbf{r}$.

The last case to consider is a magnetic source dipole at $\mathbf{r}'$ and the magnetic field to be evaluated at $\mathbf{r}$. The direct propagation of the magnetic field from the dipole to $\mathbf{r}$ is described by G_H^h. Objects of dielectric type, however, react to electric fields. Thus the second term in (3.4) has to be started from the right with $\mathrm{i}k_0 Q_{EH}^0$, giving the electric field from the magnetic dipole at $\mathbf{r}'$ at the places of the objects. $(\mathbf{1} - G_E^h V)^{-1}$ makes it the resulting electric field, V accounts for the dipole strengths of the object cells, and $-\mathrm{i}k_0 Q_{HE}^0$ propagates the magnetic field of these electric perturbation dipoles to $\mathbf{r}$.

So far, the Green's tensors in (3.1)-(3.4) have been constructed and interpreted from a physical point of view. A more formal mathematical argumentation will now be given. As already mentioned earlier, G_ε^{EE} is the tensor satisfying (2.22), which but for the δ-term and the fact that G is a tensor is the wave equation (2.6). In analogy, an equation for G_ε^{HH} is built from the wave equation for the magnetic field

$$-\nabla \wedge \frac{1}{\varepsilon(\mathbf{r})} \nabla \wedge \mathbf{H}(\mathbf{r}) + k_0^2\, \mathbf{H}(\mathbf{r}) = 0. \tag{3.5}$$

Differential equations for the mixed tensors can be based directly on Maxwell's equations (2.3, 2.4). A term $\delta(\mathbf{r} - \mathbf{r}')$ to sound out the effects of an electric type dipole source has to appear in the same place as the polarization $\mathbf{P}$. The electric field it produces is then described by G_ε^{EE} and the magnetic field entering the same equation by G_ε^{HE}. Analogously a term $\delta(\mathbf{r} - \mathbf{r}')$ in the place of a magnetization $\mathbf{M}$ goes together with the fields caused by a magnetic type dipole source given through G_ε^{HH} and G_ε^{EH}. The defining equations for the four Green's tensors are given in (3.6)-(3.9). There is no problem in G_ε^{EE} and G_ε^{HH} also appearing in the last two relations as their properties are already determined by the first two relations.

$$-\nabla \wedge \nabla \wedge G_\varepsilon^{EE}(\mathbf{r}, \mathbf{r}') \;+\; \varepsilon(\mathbf{r})\; k_0^2\; G_\varepsilon^{EE}(\mathbf{r}, \mathbf{r}') = \\ -\; 4\pi\; k_0^2\; \mathbf{1}\; \delta(\mathbf{r} - \mathbf{r}') \tag{3.6}$$

$$-\nabla \wedge \frac{1}{\varepsilon(\mathbf{r})} \nabla \wedge G_\varepsilon^{HH}(\mathbf{r}, \mathbf{r}') \;+\; k_0^2\; G_\varepsilon^{HH}(\mathbf{r}, \mathbf{r}') = \\ -\; 4\pi\; k_0^2\; \mathbf{1}\; \delta(\mathbf{r} - \mathbf{r}') \tag{3.7}$$

$$\nabla \wedge G_\varepsilon^{HE}(\mathbf{r}, \mathbf{r}') \;+\; \mathrm{i}\; k_0\; \varepsilon(\mathbf{r})\; G_\varepsilon^{EE}(\mathbf{r}, \mathbf{r}') = \\ -\; 4\pi\; \mathrm{i}\; k_0\; \mathbf{1}\; \delta(\mathbf{r} - \mathbf{r}') \tag{3.8}$$

$$\nabla \wedge G_\varepsilon^{EH}(\mathbf{r}, \mathbf{r}') \;-\; \mathrm{i}\; k_0\; G_\varepsilon^{HH}(\mathbf{r}, \mathbf{r}') = \\ 4\pi\; \mathrm{i}\; k_0\; \mathbf{1}\; \delta(\mathbf{r} - \mathbf{r}'). \tag{3.9}$$

The proof for the mathematical correctness of the tensors (3.1)-(3.4) consists in verifying that they satisfy (3.6)-(3.9). That G_ε^{EE} solves (3.6) is discussed in detail in [6]. The essential step is to replace the double rotation acting on G_E^h in both terms of G_ε^{EE} by using (2.7) resp. (A.3). The proof that G_ε^{HH} from (3.4) fulfills (3.7) is presented in Appendix B; the deduction is complicated by the position depending function $1/\varepsilon(\mathbf{r})$ between the two derivatives. The equations for the mixed tensors can be verified in a very similar manner also by making use of (A.3)-(A.10).

The tensors G_ε^{EE}, G_ε^{HE}, G_ε^{EH} and G_ε^{HH} give susceptibilities with all interactions *via* the objects present included. They describe the reaction of the system to external charges, currents or magnetizations which are not included in $\mathbf{D} = \varepsilon\mathbf{E}$ and $\mathbf{B} = \mu\mathbf{H}$ (equations in this section are for $\mu = 1$ everywhere). So if instead of (2.6) and (2.4) we have

$$-\nabla \wedge \nabla \wedge \mathbf{E}_1(\mathbf{r}) + \varepsilon(\mathbf{r})k_0^2\mathbf{E}_1(\mathbf{r}) = -4\pi k_0^2\mathbf{P}_{ext}(\mathbf{r}) \quad (3.10)$$

$$\nabla \wedge \mathbf{H}_1(\mathbf{r}) + \mathrm{i}k_0\varepsilon(\mathbf{r})\mathbf{E}_1(\mathbf{r}) = -4\pi\mathrm{i}k_0\mathbf{P}_{ext}(\mathbf{r}) \quad (3.11)$$

the solutions for the fields are

$$\mathbf{E}_1(\mathbf{r}) = \mathbf{E}^b(\mathbf{r}) + \int G_\varepsilon^{EE}(\mathbf{r},\mathbf{r}')\mathbf{P}_{ext}(\mathbf{r}')\mathrm{d}\mathbf{r}' \quad (3.12)$$

$$\mathbf{H}_1(\mathbf{r}) = \mathbf{H}^b(\mathbf{r}) + \int G_\varepsilon^{HE}(\mathbf{r},\mathbf{r}')\mathbf{P}_{ext}(\mathbf{r}')\mathrm{d}\mathbf{r}' \quad (3.13)$$

where $\mathbf{E}^b(\mathbf{r})$ and $\mathbf{H}^b(\mathbf{r})$ are the fields $\mathbf{E}(\mathbf{r})$ and $\mathbf{H}(\mathbf{r})$ calculated in (2.18) and (2.23); they now constitute the new background from the point of view of the external polarization, as they satisfy the homogeneous differential equations, *i.e.* (3.10) and (3.11) with zero instead of $\mathbf{P}_{ext}$ on the right side.

In the same way with an external magnetization (3.5) and (2.3) get changed into

$$-\nabla \wedge \frac{1}{\varepsilon(\mathbf{r})}\nabla \wedge \mathbf{H}_2(\mathbf{r}) + k_0^2\mathbf{H}_2(\mathbf{r}) = -4\pi k_0^2\mathbf{M}_{ext}(\mathbf{r}) \quad (3.14)$$

$$\nabla \wedge \mathbf{E}_2(\mathbf{r}) - \mathrm{i}k_0\mathbf{H}_2(\mathbf{r}) = 4\pi\mathrm{i}k_0\mathbf{M}_{ext}(\mathbf{r}) \quad (3.15)$$

and solved by

$$\mathbf{E}_2(\mathbf{r}) = \mathbf{E}^b(\mathbf{r}) + \int G_\varepsilon^{EH}(\mathbf{r},\mathbf{r}')\mathbf{M}_{ext}(\mathbf{r}')\mathrm{d}\mathbf{r}' \quad (3.16)$$

$$\mathbf{H}_2(\mathbf{r}) = \mathbf{H}^b(\mathbf{r}) + \int G_\varepsilon^{HH}(\mathbf{r},\mathbf{r}')\mathbf{M}_{ext}(\mathbf{r}')\mathrm{d}\mathbf{r}'. \quad (3.17)$$

Paying attention to whether even without the excitations taken here as $\mathbf{P}_{ext}$ and $\mathbf{M}_{ext}$ there are any fields $\mathbf{E}^b(\mathbf{r})$ and $\mathbf{H}^b(\mathbf{r})$ and avoiding counting such contributions twice, the fields from (3.12) and (3.16) resp. (3.13) and (3.17) simply have to be added to get the solution for the case where both $\mathbf{P}_{ext}$ and $\mathbf{M}_{ext}$ are present at the same time.

A fully equivalent approach consists in first combining the external excitations as they would appear together in the wave equations for the electric and the magnetic field and then using only the pure electric and pure magnetic Green's tensors to evaluate the resulting fields. One then gets

$$-\nabla \wedge \nabla \wedge \mathbf{E}(\mathbf{r}) + \varepsilon(\mathbf{r})k_0^2\mathbf{E}(\mathbf{r}) = -4\pi k_0^2\mathbf{Q}_1(\mathbf{r}) \quad (3.18)$$

$$-\nabla \wedge \frac{1}{\varepsilon(\mathbf{r})}\nabla \wedge \mathbf{H}(\mathbf{r}) + k_0^2\mathbf{H}(\mathbf{r}) = -4\pi k_0^2\mathbf{Q}_2(\mathbf{r}) \quad (3.19)$$

with

$$\mathbf{Q}_1(\mathbf{r}) = \mathbf{P}_{ext}(\mathbf{r}) + \frac{\mathrm{i}}{k_0}\nabla \wedge \mathbf{M}_{ext}(\mathbf{r}) \quad (3.20)$$

$$\mathbf{Q}_2(\mathbf{r}) = \mathbf{M}_{ext}(\mathbf{r}) - \frac{\mathrm{i}}{k_0}\nabla \wedge \frac{\mathbf{P}_{ext}(\mathbf{r})}{\varepsilon(\mathbf{r})} \quad (3.21)$$

which are solved by

$$\mathbf{E}(\mathbf{r}) = \mathbf{E}^b(\mathbf{r}) + \int G_\varepsilon^{EE}(\mathbf{r},\mathbf{r}')\mathbf{Q}_1(\mathbf{r}')\mathrm{d}\mathbf{r}' \quad (3.22)$$

$$\mathbf{H}(\mathbf{r}) = \mathbf{H}^b(\mathbf{r}) + \int G_\varepsilon^{HH}(\mathbf{r},\mathbf{r}')\mathbf{Q}_2(\mathbf{r}')\mathrm{d}\mathbf{r}'. \quad (3.23)$$

4 Magnetic perturbations

The situation that the objects only have magnetic permeabilities but no dielectric permeabilities differing from the background is mathematically fully equivalent to the one discussed in the last sections. The roles of the electric and the magnetic field get interchanged. In analogy to V we build the matrix M. The elements of M are zero but for 3×3-blocks on the diagonal which are taken to be the susceptibility tensors $\frac{\mu(\mathbf{r})-1}{4\pi}$ of the perturbation cells multiplied by the volume $\triangle v$ of the cells. The four Green's tensors in this case are

$$G_\mu^{HH} = G_H^h + G_H^h M(\mathbf{1} - G_H^h M)^{-1}G_H^h \quad (4.1)$$

$$G_\mu^{EH} = \mathrm{i}k_0 Q_{EH}^0 + \mathrm{i}k_0 Q_{EH}^0 M(\mathbf{1} - G_H^h M)^{-1}G_H^h \quad (4.2)$$

$$G_\mu^{HE} = -\mathrm{i}k_0 Q_{HE}^0 - \mathrm{i}k_0 G_H^h M(\mathbf{1} - G_H^h M)^{-1}Q_{HE}^0 \quad (4.3)$$

$$G_\mu^{EE} = G_E^h + k_0^2 Q_{EH}^0 M(\mathbf{1} - G_H^h M)^{-1}Q_{HE}^0 \quad (4.4)$$

and satisfy

$$-\nabla \wedge \nabla \wedge G_\mu^{HH}(\mathbf{r},\mathbf{r}') \; + \; \mu(\mathbf{r})\; k_0^2\; G_\mu^{HH}(\mathbf{r},\mathbf{r}') = - 4\pi\; k_0^2\; \mathbf{1}\; \delta(\mathbf{r}-\mathbf{r}') \quad (4.5)$$

$$-\nabla \wedge \frac{1}{\mu(\mathbf{r})}\nabla \wedge G_\mu^{EE}(\mathbf{r},\mathbf{r}') \; + \; k_0^2\; G_\mu^{EE}(\mathbf{r},\mathbf{r}') = - 4\pi\; k_0^2\; \mathbf{1}\; \delta(\mathbf{r}-\mathbf{r}') \quad (4.6)$$

$$\nabla \wedge G_\mu^{EH}(\mathbf{r},\mathbf{r}') \; - \; \mathrm{i}\; k_0\; \mu(\mathbf{r})\; G_\mu^{HH}(\mathbf{r},\mathbf{r}') = 4\pi\; \mathrm{i}\; k_0\; \mathbf{1}\; \delta(\mathbf{r}-\mathbf{r}') \quad (4.7)$$

$$\nabla \wedge G_\mu^{HE}(\mathbf{r},\mathbf{r}') \; + \; \mathrm{i}\; k_0\; G_\mu^{EE}(\mathbf{r},\mathbf{r}') = - 4\pi\; \mathrm{i}\; k_0\; \mathbf{1}\; \delta(\mathbf{r}-\mathbf{r}'). \quad (4.8)$$

5 Total Green's tensors

In general, the objects (Fig. 1) may have dielectric as well as magnetic permeabilities and Green's tensors for this case will now be searched. If neither ε nor μ is unity everywhere, the wave equations for the two fields and the two Maxwell relations containing the curl read

$$-\nabla \wedge \frac{1}{\mu(\mathbf{r})}\nabla \wedge \mathbf{E}(\mathbf{r}) + \varepsilon(\mathbf{r})\ k_0^2\ \mathbf{E}(\mathbf{r}) = 0 \tag{5.1}$$

$$-\nabla \wedge \frac{1}{\varepsilon(\mathbf{r})}\nabla \wedge \mathbf{H}(\mathbf{r}) + \mu(\mathbf{r})\ k_0^2\ \mathbf{H}(\mathbf{r}) = 0 \tag{5.2}$$

$$\nabla \wedge \mathbf{H}\ + \mathrm{i}k_0\ \varepsilon(\mathbf{r})\ \mathbf{E}(\mathbf{r}) = 0 \tag{5.3}$$

$$\nabla \wedge \mathbf{E}\ - \mathrm{i}k_0\ \mu(\mathbf{r})\ \mathbf{H}(\mathbf{r}) = 0. \tag{5.4}$$

To derive defining equations for the tensors G_{tot}^{EE} and G_{tot}^{HE} describing the reaction of the system to an electric dipole source, besides replacing the fields by tensors the recipe is to make a point source appear in parallel to the polarization term $\varepsilon\mathbf{E}$ in (5.1) and (5.3). Equations for the tensors G_{tot}^{HH} and G_{tot}^{EH} giving the reaction to a magnetic dipole source are constructed by placing a point source in parallel to the magnetization term $\mu\mathbf{H}$ in (5.2) and (5.4). Thus the equations to solve in order to find the total Green's tensors are

$$-\nabla \wedge \frac{1}{\mu(\mathbf{r})}\nabla \wedge G_{tot}^{EE}(\mathbf{r},\mathbf{r}') + \varepsilon(\mathbf{r})\ k_0^2\ G_{tot}^{EE}(\mathbf{r},\mathbf{r}') = -4\pi\ k_0^2\ \mathbf{1}\ \delta(\mathbf{r}-\mathbf{r}') \tag{5.5}$$

$$-\nabla \wedge \frac{1}{\varepsilon(\mathbf{r})}\nabla \wedge G_{tot}^{HH}(\mathbf{r},\mathbf{r}') + \mu(\mathbf{r})\ k_0^2\ G_{tot}^{HH}(\mathbf{r},\mathbf{r}') = -4\pi\ k_0^2\ \mathbf{1}\ \delta(\mathbf{r}-\mathbf{r}') \tag{5.6}$$

$$\nabla \wedge G_{tot}^{HE}(\mathbf{r},\mathbf{r}') + \mathrm{i}\ k_0\ \varepsilon(\mathbf{r})\ G_{tot}^{EE}(\mathbf{r},\mathbf{r}') = -4\pi\ \mathrm{i}\ k_0\ \mathbf{1}\ \delta(\mathbf{r}-\mathbf{r}') \tag{5.7}$$

$$\nabla \wedge G_{tot}^{EH}(\mathbf{r},\mathbf{r}') - \mathrm{i}\ k_0\ \mu(\mathbf{r})\ G_{tot}^{HH}(\mathbf{r},\mathbf{r}') = 4\pi\ \mathrm{i}\ k_0\ \mathbf{1}\ \delta(\mathbf{r}-\mathbf{r}'). \tag{5.8}$$

The first one, equation (5.5), is also found in reference [7], however, an explicit solution for arbitrary three-dimensional geometries has so far only been given for (3.6) or (5.5) with constant μ. Comparing (5.5) to (3.6) from Section 3, the difficulty in finding G_{tot}^{EE} now is the function $1/\mu(\mathbf{r})$ between the derivatives. Nevertheless, an ansatz in the same form as (2.19)

$$G_{tot}^{EE} = G^* + G^*\ V\ (\mathbf{1} - G^*V)^{-1}\ G^* \tag{5.9}$$

with some yet unknown tensor G^* is successful. It turns out that G_{tot}^{EE} satisfies (5.5) if G^* is taken to be G_{μ}^{EE} from (4.4).

Analyzing the building scheme of G_{tot}^{EE} helps to infer the other tensors by "educated guess". In G_{tot}^{EE}, the effect of dielectric permeabilities of the objects is described by the "convolution" with V in the form (5.9). Instead of G_E^h as in (3.1) there is now G_{μ}^{EE}, already accounting for magnetic permeabilities of the objects, as the "background". G_{tot}^{EE} could also have been constructed the other way round by first evaluating the Green's tensors from Section 3 only involving the dielectric permeabilities and then inserting them in the expression from (4.4) to replace the background tensors G_E^h, G_H^h, Q_{HE}^0 and Q_{EH}^0. Analogously I infer two forms for each of the other three tensors G_{tot}^{HH}, G_{tot}^{HE} and G_{tot}^{EH} as well.

$$G_{tot}^{EE} = G_{\mu}^{EE} + G_{\mu}^{EE}V(\mathbf{1} - G_{\mu}^{EE}V)^{-1}G_{\mu}^{EE} \tag{5.10a}$$
$$= G_{\varepsilon}^{EE} + G_{\varepsilon}^{EH}M(\mathbf{1} - G_{\varepsilon}^{HH}M)^{-1}G_{\varepsilon}^{HE} \tag{5.10b}$$

$$G_{tot}^{HH} = G_{\mu}^{HH} + G_{\mu}^{HE}V(\mathbf{1} - G_{\mu}^{EE}V)^{-1}G_{\mu}^{EH} \tag{5.11a}$$
$$= G_{\varepsilon}^{HH} + G_{\varepsilon}^{HH}M(\mathbf{1} - G_{\varepsilon}^{HH}M)^{-1}G_{\varepsilon}^{HH} \tag{5.11b}$$

$$G_{tot}^{HE} = G_{\mu}^{HE} + G_{\mu}^{HE}V(\mathbf{1} - G_{\mu}^{EE}V)^{-1}G_{\mu}^{EE} \tag{5.12a}$$
$$= G_{\varepsilon}^{HE} + G_{\varepsilon}^{HH}M(\mathbf{1} - G_{\varepsilon}^{HH}M)^{-1}G_{\varepsilon}^{HE} \tag{5.12b}$$

$$G_{tot}^{EH} = G_{\mu}^{EH} + G_{\mu}^{EE}V(\mathbf{1} - G_{\mu}^{EE}V)^{-1}G_{\mu}^{EH} \tag{5.13a}$$
$$= G_{\varepsilon}^{EH} + G_{\varepsilon}^{EH}M(\mathbf{1} - G_{\varepsilon}^{HH}M)^{-1}G_{\varepsilon}^{HH}. \tag{5.13b}$$

That these tensors in both their forms indeed satisfy (5.5)-(5.8), can be checked by calculations similar to the one in Appendix B, by inserting the tensors and making use of the known properties (A.3)-(A.10), (3.6)-(3.9) and (4.5)-(4.8). The simpler tensors from Sections 3 and 4, of course, are just specific cases of the ones here. I shall end this section with a few more remarks on the construction of the general Green's tensors and their meaning.

For the simplest case with a completely homogeneous background G_E^h and G_H^h resp. Q_{HE}^0 and Q_{EH}^0 are identical. And if the presence of a substrate surface is accounted for in the electrostatic approximation, Q_{HE}^0 and Q_{EH}^0 are still the same tensor even in this case. The indices in (3.1)-(3.4) and (4.1)-(4.4) nevertheless help to remember whether a G^h meant the background propagator of the electric or the magnetic field and whether a Q^0 was implied to calculate the magnetic field of an electric dipole or the electric field of a magnetic dipole. So the indices of the background tensors in (3.1)-(3.4) resp. (4.1)-(4.4) tell us by which tensor from (4.1)-(4.4) resp. (3.1)-(3.4) each one has to be replaced to get the generalizations (5.10)-(5.13).

It is of no importance whether a discretization cell of the objects is ascribed only an $\varepsilon \neq 1$, only a $\mu \neq 1$ or both. As explained in Sections 2 and 4, V is the matrix with the dielectric susceptibilities $\chi = \frac{\varepsilon-1}{4\pi}$ and M is the matrix with the magnetic susceptibilities $\frac{\mu-1}{4\pi}$ as diagonal elements. There may be object cell coordinates figuring in both or not. Every tensor contraction with V is over all cells with $\varepsilon \neq 1$, and every tensor contraction with M is over all cells with $\mu \neq 1$.

The following argument is to show for G_{tot}^{EE} as an example that the two forms for each tensor in (5.10)-(5.13) really give the same tensor. The identity is not obvious even if the expressions from (3.1)-(3.4) and (4.1)-(4.4) are

substituted for the tensors indexed ε resp. μ.

$$\begin{aligned} G_{tot}^{EE} &= G_E^h + k_0^2 Q_{EH}^0 M(\mathbf{1} - G_H^h M)^{-1} Q_{HE}^0 \\ &\quad + (G_E^h + k_0^2 Q_{EH}^0 M(\mathbf{1} - G_H^h M)^{-1} Q_{HE}^0)V \\ &\quad \times [\mathbf{1} - (G_E^h + k_0^2 Q_{EH}^0 M(\mathbf{1} - G_H^h M)^{-1} Q_{HE}^0)V]^{-1} \\ &\quad \times (G_E^h + k_0^2 Q_{EH}^0 M(\mathbf{1} - G_H^h M)^{-1} Q_{HE}^0) \qquad (5.14a) \\ &= G_E^h + G_E^h V(\mathbf{1} - G_E^h V)^{-1} G_E^h \\ &\quad + (\mathrm{i}k_0 Q_{EH}^0 + \mathrm{i}k_0 G_E^h V(\mathbf{1} - G_E^h V)^{-1} Q_{EH}^0)M \\ &\quad \times [\mathbf{1} - (G_H^h + k_0^2 Q_{HE}^0 V(\mathbf{1} - G_E^h V)^{-1} Q_{EH}^0)M]^{-1} \\ &\quad \times (-\mathrm{i}k_0 Q_{HE}^0 - \mathrm{i}k_0 Q_{HE}^0 V(\mathbf{1} - G_E^h V)^{-1} G_E^h). \qquad (5.14b) \end{aligned}$$

Yet consider developing all $(\ldots)^{-1}$ into infinite series following the pattern of (2.20). For both forms of G_{tot}^{EE} this will result in

$$\begin{aligned} G_{tot}^{EE} = {} & G_E^h + G_E^h V G_E^h + k_0 Q_{EH}^0 M k_0 Q_{HE}^0 \\ & + G_E^h V G_E^h V G_E^h \\ & + G_E^h V k_0 Q_{EH}^0 M k_0 Q_{HE}^0 \\ & + k_0 Q_{EH}^0 M k_0 Q_{HE}^0 V G_E^h \\ & + k_0 Q_{EH}^0 M G_H^h M k_0 Q_{HE}^0 + \ldots \qquad (5.15) \end{aligned}$$

where there is no difference any more between the levels at which V and M occur. The recipe to construct this infinite series is the following: Start with G_E^h. Products with $n+1$ tensors G^h or Q^0 can be deduced from the ones with n tensors. For an n-product ending with G_E^h you get one $n+1$-product where simply VG_E^h is appended and one $n+1$-product where the last G_E^h is changed into $k_0 Q_{EH}^0$ and $Mk_0 Q_{HE}^0$ is appended. For an n-product ending with $k_0 Q_{HE}^0$ you get one $n+1$-product where VG_E^h is appended and one $n+1$-product where the last $k_0 Q_{HE}^0$ is changed into G_H^h and then $Mk_0 Q_{HE}^0$ is appended. (In G_{tot}^{EE} all terms begin with G_E^h or $k_0 Q_{EH}^0$ and end with G_E^h or $k_0 Q_{HE}^0$.) In this scheme all electric and magnetic interactions to all orders are successively added up. In the same way, to see the equivalence of the two forms for G_{tot}^{HH}, G_{tot}^{HE} and G_{tot}^{EH}, imagine all tensors indexed ε and μ in (5.10)-(5.13) substituted by their elementary representations and all $(\ldots)^{-1}$ developed into series. The convergence of infinite series like (5.15) has not been investigated, and for model calculations the compact forms (5.10)-(5.13) with matrix inversions are taken, of course.

For fixed arguments $\mathbf{r}$ and $\mathbf{r}'$ the Green's tensors $G^{EE}(\mathbf{r},\mathbf{r}')$, $G^{HH}(\mathbf{r},\mathbf{r}')$, $G^{HE}(\mathbf{r},\mathbf{r}')$ and $G^{EH}(\mathbf{r},\mathbf{r}')$, whether indexed ε for dielectric perturbations, μ for magnetic perturbations or *tot* for both, are 3×3 matrices with complex elements. Quantities accessible to measurement are correlation functions between field components and these are given by the imaginary parts of the pure tensors G^{EE} and G^{HH} and by the real parts of the mixed tensors G^{HE} and G^{EH} [31]. For identical arguments $\mathbf{r}'=\mathbf{r}$ the imaginary parts of the diagonal elements resp. of the trace of G^{EE} give the partial resp. total local densities of states (LDOS) of the electric field [6,19,20,24,32]. The imaginary parts of the diagonal elements resp. of the trace of G^{HH} analogously represent the partial resp. total local densities of states of the magnetic field. The mixed susceptibility tensors, however, can only be interpreted as response functions.

6 Field distributions

Of course, the fields can be calculated by first evaluating the total Green's tensors and then, generalizing (2.18), building

$$\begin{aligned} \mathbf{E}(\mathbf{r}) = \mathbf{E}^0(\mathbf{r}) &+ \int_A G_{tot}^{EE}(\mathbf{r},\mathbf{r}')\frac{\varepsilon(\mathbf{r}')-1}{4\pi}\mathbf{E}^0(\mathbf{r}')\mathrm{d}\mathbf{r}' \\ &+ \int_{A'} G_{tot}^{EH}(\mathbf{r},\mathbf{r}')\frac{\mu(\mathbf{r}')-1}{4\pi}\mathbf{H}^0(\mathbf{r}')\mathrm{d}\mathbf{r}' \qquad (6.1) \\ \mathbf{H}(\mathbf{r}) = \mathbf{H}^0(\mathbf{r}) &+ \int_A G_{tot}^{HE}(\mathbf{r},\mathbf{r}')\frac{\varepsilon(\mathbf{r}')-1}{4\pi}\mathbf{E}^0(\mathbf{r}')\mathrm{d}\mathbf{r}' \\ &+ \int_{A'} G_{tot}^{HH}(\mathbf{r},\mathbf{r}')\frac{\mu(\mathbf{r}')-1}{4\pi}\mathbf{H}^0(\mathbf{r}')\mathrm{d}\mathbf{r}' \qquad (6.2) \end{aligned}$$

with $\mathbf{E}^0(\mathbf{r})$ and $\mathbf{H}^0(\mathbf{r})$ the initial fields from a source or an incident wave, A the region where $\varepsilon \neq 1$ and A' the region where $\mu \neq 1$. However, if we are only interested in maps of field distributions, the explicit calculation of all the total Green's tensors can be avoided. As done in Section 2 for the electric field with dielectric objects, you can just solve implicit Lippmann-Schwinger equations for the fields inside the perturbations and then propagate these by the free space Green's tensors to the locations of interest. In the general case with perturbations with $\varepsilon \neq 1$ and $\mu \neq 1$ instead of (2.11) there are two interlinked implicit equations:

$$\begin{aligned} \mathbf{E}(\mathbf{r}) = \mathbf{E}^0(\mathbf{r}) &+ \int_A G_E^h(\mathbf{r},\mathbf{r}')\frac{\varepsilon(\mathbf{r}')-1}{4\pi}\mathbf{E}(\mathbf{r}')\mathrm{d}\mathbf{r}' \\ &+ \mathrm{i}k_0 \int_{A'} Q_{EH}^0(\mathbf{r},\mathbf{r}')\frac{\mu(\mathbf{r}')-1}{4\pi}\mathbf{H}(\mathbf{r}')\mathrm{d}\mathbf{r}' \qquad (6.3) \\ \mathbf{H}(\mathbf{r}) = \mathbf{H}^0(\mathbf{r}) &- \mathrm{i}k_0 \int_A Q_{HE}^0(\mathbf{r},\mathbf{r}')\frac{\varepsilon(\mathbf{r}')-1}{4\pi}\mathbf{E}(\mathbf{r}')\mathrm{d}\mathbf{r}' \\ &+ \int_{A'} G_H^h(\mathbf{r},\mathbf{r}')\frac{\mu(\mathbf{r}')-1}{4\pi}\mathbf{H}(\mathbf{r}')\mathrm{d}\mathbf{r}'. \qquad (6.4) \end{aligned}$$

Numbering $1,\ldots,N$ the cells with $\varepsilon \neq 1$ and their locations $\mathbf{r}_1,\ldots,\mathbf{r}_N$, and counting $1,\ldots,M$ the cells with $\mu \neq 1$ and their locations $\mathbf{r'}_1,\ldots,\mathbf{r'}_M$, in the discretization these equations become

$$\begin{aligned} \mathbf{E}(\mathbf{r}_n) = \mathbf{E}^0(\mathbf{r}_n) &+ \sum_{n'=1}^{N} G_E^h(\mathbf{r}_n,\mathbf{r}_{n'})\frac{\varepsilon(\mathbf{r}_{n'})-1}{4\pi}\mathbf{E}(\mathbf{r}_{n'})\triangle v \\ &+ \mathrm{i}k_0 \sum_{m'=1}^{M} Q_{EH}^0(\mathbf{r}_n,\mathbf{r'}_{m'})\frac{\mu(\mathbf{r'}_{m'})-1}{4\pi}\mathbf{H}(\mathbf{r'}_{m'})\triangle v \qquad (6.5) \end{aligned}$$

$$\mathbf{H}(\mathbf{r'}_m) = \mathbf{H}^0(\mathbf{r'}_m) - \mathrm{i}k_0 \sum_{n'=1}^{N} Q^0_{HE}(\mathbf{r'}_m, \mathbf{r}_{n'}) \frac{\varepsilon(\mathbf{r}_{n'}) - 1}{4\pi} \mathbf{E}(\mathbf{r}_{n'}) \triangle v + \sum_{m'=1}^{M} G^h_H(\mathbf{r'}_m, \mathbf{r'}_{m'}) \frac{\mu(\mathbf{r'}_{m'}) - 1}{4\pi} \mathbf{H}(\mathbf{r'}_{m'}) \triangle v. \quad (6.6)$$

There may be vectors appearing in $\mathbf{r}_1, \ldots, \mathbf{r}_N$ as well as in $\mathbf{r'}_1, \ldots, \mathbf{r'}_M$. If a cell has $\varepsilon \neq 1$ and $\mu \neq 1$ it is counted as an electric dipole and a magnetic dipole. For the formalism, it is of no importance if these are at the same place or not. (6.5) and (6.6) constitute a system of linear equations for all the $\mathbf{E}(\mathbf{r}_n)$ and $\mathbf{H}(\mathbf{r'}_m)$. To solve it, build one long vector out of all the $\mathbf{E}^0(\mathbf{r}_n)$ and $\mathbf{H}^0(\mathbf{r'}_m)$, one long vector out of all the $\mathbf{E}(\mathbf{r}_n)$ and $\mathbf{H}(\mathbf{r'}_m)$, as well as a four quadrant matrix of all the coefficients. Then (6.5) and (6.6) can be written as

$$\begin{pmatrix} \mathbf{1} - G^h_E V & -\mathrm{i}k_0 Q^0_{EH} M \\ \mathrm{i}k_0 Q^0_{HE} V & \mathbf{1} - G^h_H M \end{pmatrix} \begin{pmatrix} E_A \\ H_{A'} \end{pmatrix} = \begin{pmatrix} E^0_A \\ H^0_{A'} \end{pmatrix}. \quad (6.7)$$

You get E_A and $H_{A'}$ inside the perturbation by inverting this matrix

$$\begin{pmatrix} E_A \\ H_{A'} \end{pmatrix} = \begin{pmatrix} \mathbf{1} - G^h_E V & -\mathrm{i}k_0 Q^0_{EH} M \\ \mathrm{i}k_0 Q^0_{HE} V & \mathbf{1} - G^h_H M \end{pmatrix}^{-1} \begin{pmatrix} E^0_A \\ H^0_{A'} \end{pmatrix} \quad (6.8)$$

and then the fields elsewhere can be evaluated from (6.3) and (6.4) with $\mathbf{r}$ outside the perturbations.

$$E_B = E^0_B + G^h_{E,BA} V_A E_A + \mathrm{i}k_0 Q^0_{EH,BA'} M_{A'} H_{A'} \quad (6.9)$$

$$H_B = H^0_B - \mathrm{i}k_0 Q^0_{HE,BA} V_A E_A + G^h_{H,BA'} M_{A'} H_{A'}. \quad (6.10)$$

The indices A, A' and B in (6.9) and (6.10) indicate the region the arguments of the fields and tensors belong to. (6.9) and (6.10) together with (6.8) are equivalent to (6.1) and (6.2), but much easier to implement.

7 Examples

In the first part of this section as quite basic examples of calculated field maps I consider just one square-shaped pad on a surface illuminated in total internal reflection (Fig. 2). In Figure 3 the particle is dielectric with the same isotropic ε as the substrate. Field maps in a plane shortly above the particle show the following features [25]: For s-polarization the pad appears as a dark contrast in the electric field intensity with intensity enhancements at the sides where there are strong field gradients. The magnetic field intensity has an a little blurred out bright contrast directly above the pad. For p-polarization the electric field intensity is well confined above the pad whereas in the magnetic field intensity the pad appears as a dark contrast with comparatively widespread enhancements above the edges perpendicular to the direction of propagation of the incident wave.

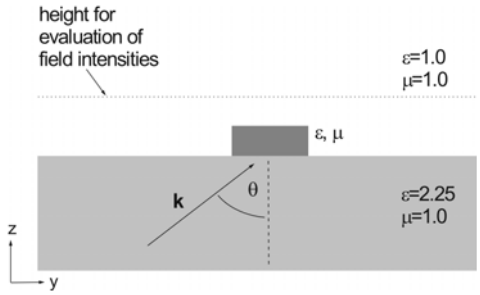

Fig. 2. Model structure for calculations of field distributions shown in Figures 3–6: a square pad, 90 nm in x- and y-direction, 30 nm in z-direction, on a glass substrate. The perturbation is discretized into an array of 3×3 cubes of edge 30 nm which are each ascribed ε and μ. The system is illuminated by a linearly polarized plane wave in total internal reflection ($\theta = 60°$) at vacuum wavelength $\lambda = 633$ nm. Intensities of the electric and the magnetic field are evaluated in a plane 50 nm above the substrate.

Next I investigate a pad that has a magnetic, but no dielectric susceptibility (Fig. 4). Compared to Figure 3, essentially the patterns of the electric and the magnetic field intensities as well as the ones for s- and p-polarization get interchanged. The configuration is not absolutely equivalent to Figure 3 though, as the pad is magnetic instead of dielectric, but the substrate is still dielectric. Small differences in the field patterns between Figures 3 and 4 are due to this fact.

For the calculations in Figure 5 the pad was supposed to have a dielectric as well as a magnetic susceptibility. The strongest features that Figures 3 and 4 have in common are reproduced, namely the pad appearing bright in $|\mathbf{E}|^2$ for p-polarization and in $|\mathbf{H}|^2$ for s-polarization resp. appearing dark in $|\mathbf{E}|^2$ for s-polarization and in $|\mathbf{H}|^2$ for p-polarization. Furthermore, $|\mathbf{E}|^2$ for s-polarization and $|\mathbf{H}|^2$ for p-polarization resp. $|\mathbf{E}|^2$ for p-polarization and $|\mathbf{H}|^2$ for s-polarization are very similar to one another. This will no longer be the case and the field patterns will get more complicated if the dielectric and the magnetic susceptibility are not chosen of equal strength.

Contrarily to dielectric permeabilities efficient magnetic susceptibilities at optical frequencies are normally not provided by atomic or pure material properties. Surface plasmon polariton eigenmodes of cylindrical metallic structures of the dimensions of optical wavelengths, however, build up electric and magnetic dipole moments of comparable strengths or even a magnetic dipole moment exceeding the electric one. For the plasmon mode of interest (labeled $n = 1$ in [27]) the electric as well as the magnetic dipole moment are perpendicular to the cylinder axis. Therefore, having in mind to give a first very simple near-field model for objects potentially exhibiting magnetic susceptibilities, *i.e.* rings lying on a surface or cylindrical holes in metal films [33], in Figure 6 the calculations from Figure 5 are repeated with non-isotropic susceptibilities for the pad.

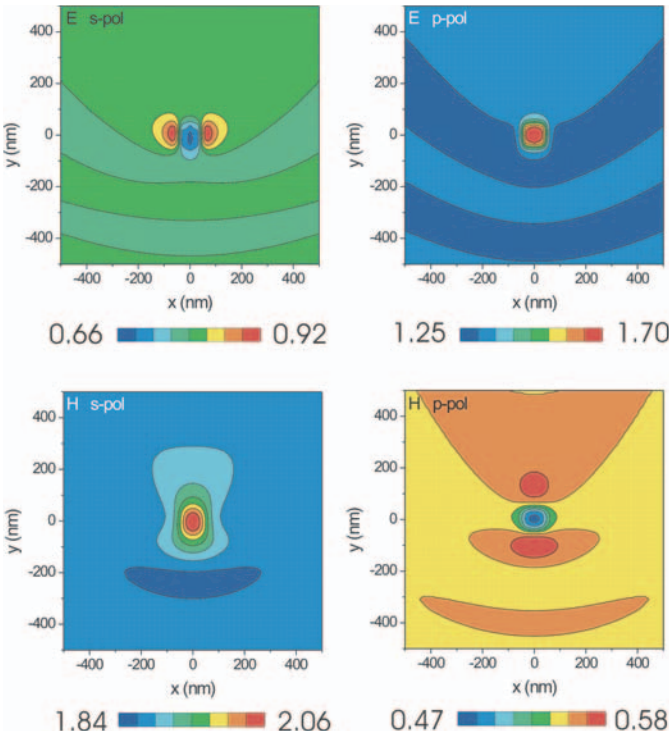

Fig. 3. Field intensity maps showing $|\mathbf{E}|^2$ and $|\mathbf{H}|^2$ above the object depicted in Figure 2 for both polarizations of the incident light. The pad material has $\varepsilon = 2.25$ and $\mu = 1$ (no imaginary parts) like the substrate. The origin $x = 0$ and $y = 0$ is above the center of the pad and the propagation along y of the incident wave is from bottom to top in Figures 3–6. The normalization is $|\mathbf{E}_0| \equiv 1$ for the incident wave below the surface; in cgs $\mathbf{E}$ and $\mathbf{H}$ have the same units.

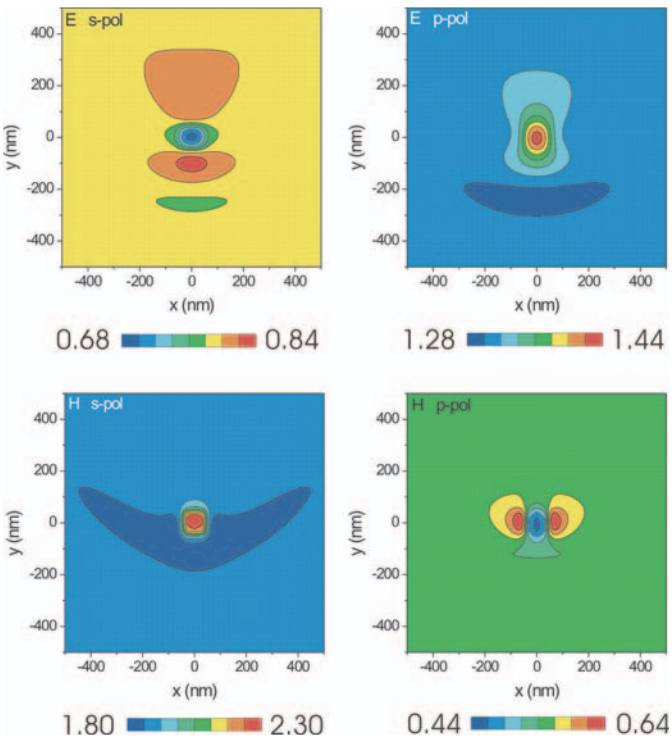

Fig. 4. Same as Figure 3, except that now the material of the pad has $\varepsilon = 1.0$ and $\mu = 2.25$.

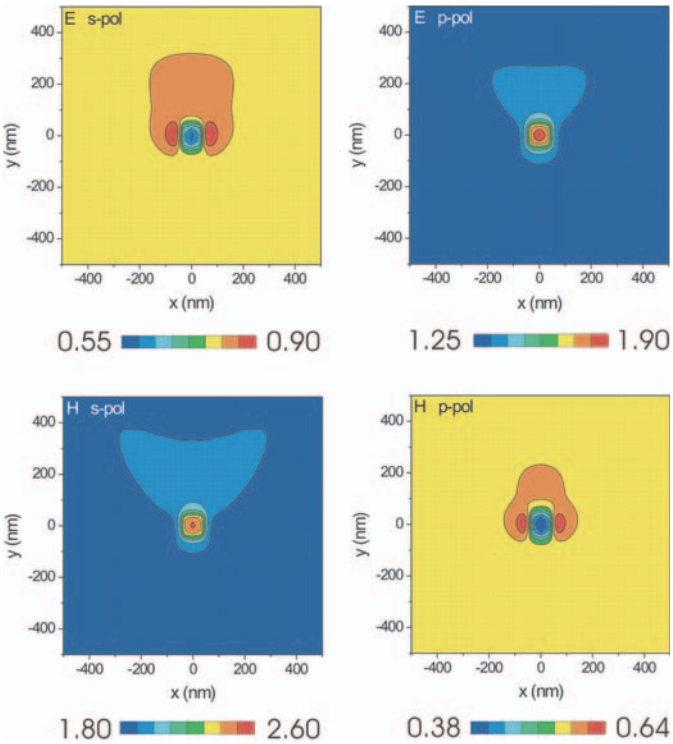

Fig. 5. Like Figures 3 and 4, but with pad material $\varepsilon = 2.25$ and $\mu = 2.25$.

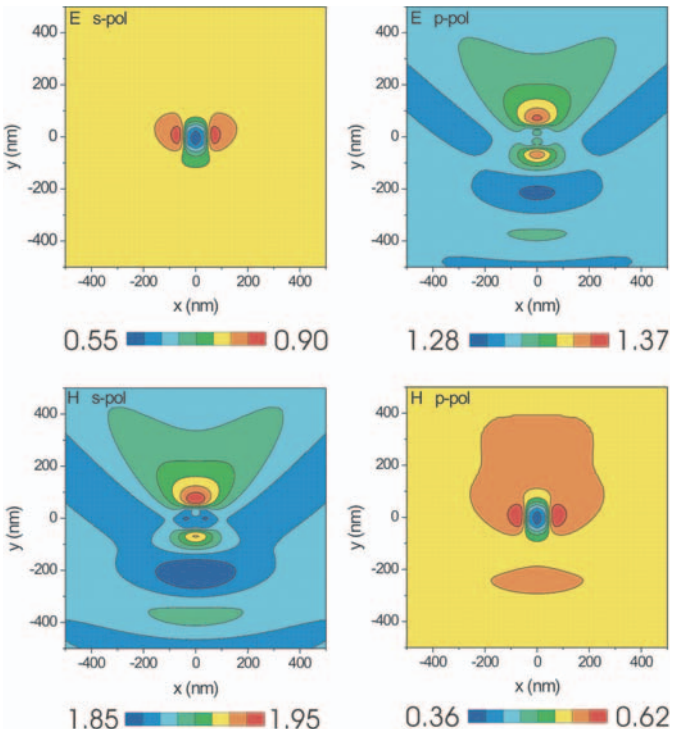

Fig. 6. Like Figure 5, but with anisotropic pad material; $\varepsilon_x = \varepsilon_y = 2.25$, $\varepsilon_z = 1.0$ and $\mu_x = \mu_y = 2.25$, $\mu_z = 1.0$.

The missing susceptibilities in z-direction lead to differences in the field patterns compared to Figure 5, especially for those fields for which the incident wave contains a z-component, that is **E** for p-polarization and **H** for s-polarization. There no longer is an enhanced z-component directly above the pad much larger in intensity than the smaller scale contrasts around the pad. Field patterns analogous to the ones from Figure 6 will also become more complex and of greater variety, if ε and μ of the object are well of the same order, but no longer of equal weight. Whereas contrasts and patterns get (inter-)changed, the intensities remain in the same orders of magnitude throughout Figures 3 to 6; absolute signal calibration, however, is often not available in NSOM setup.

The second part of this section is on the different Green's tensors for the stadium structure from [20] (see Fig. 7). Although feasible in the theoretical framework developed in the preceding sections, the structure modelled here has no magnetic susceptibility. Nevertheless, as already seen from the field distributions, purely dielectric objects are also able to modify the optical magnetic field distribution in their vicinity [25]. And mixed and magnetic Green's tensor maps have not been shown so far, even for dielectric perturbations. For brevity, only the imaginary or the real part of each complex tensor component is plotted; the choice is oriented at equations (3.13)-(3.16) from [31], but is not at all meant to exclude a physical relevance of the part which is not drawn.

For comparison $\mathrm{Im}G^{EE}(\mathbf{r},\mathbf{r})$ is shown in Figure 8. The diagonal components give the partial local densities of states (LDOS) of the electric field, that is, $\mathrm{Im}G^{EE}_{xx}(\mathbf{r},\mathbf{r},\omega)$ is proportional to $\rho^E_x(\mathbf{r},\omega)$, etc. Note that the densities are given relatively to the constant value of the LDOS in vacuum [20,32]. As G^{EE} is a symmetric tensor, $G^{EE}_{ij} = G^{EE}_{ji}$, there are only three independent off-diagonal components of $\mathrm{Im}G^{EE}$, which are also drawn in Figure 8. In the patterns of the diagonal elements the actual positions of the particles are relatively well discernable. The xy-component has a rotational rather than a reflection symmetry. In the xz- and the yz-components enhancements blur out the image of the structure along the curved resp. the straight sides of the stadium, and there is much less contrast away from the particles inside as well as outside the stadium.

G^{HH} like G^{EE} is a symmetric tensor and the imaginary part of its six different components is drawn in Figure 9. In the magnetic tensor, the diagonal xx- and yy-components differ less from one another than in the electric tensor. The weaker patterns inside and outside the stadium are not identical, though. In G^{HH}_{zz} the curved and straight boundaries of the stadium give a quite unequal appearance in contrast to the rather uniform image of all particles in G^{EE}_{zz}. The off-diagonal components resemble the ones of the electric tensor.

All nine components of $\mathrm{Re}G^{EH}(\mathbf{r},\mathbf{r})$ are plotted in Figure 10. The mixed Green's tensors are not symmetric and although in our example the most dominant features in the images are found with inverted contrast in

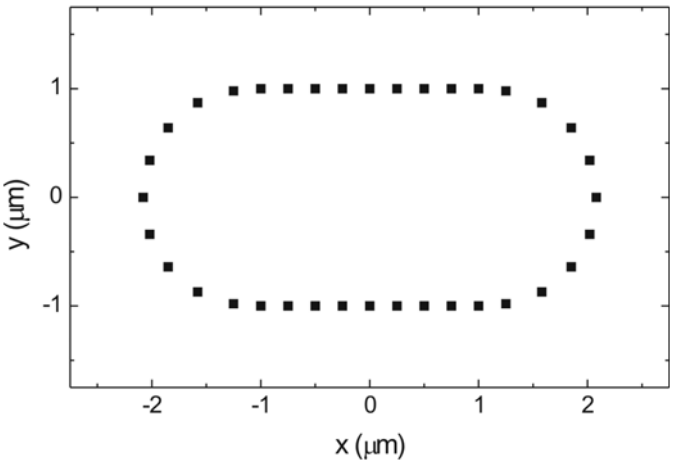

Fig. 7. Model structure for calculations of Green's tensors consisting of 36 metal particles on a glass surface ($\varepsilon = 2.25$). Each particle is 90 nm × 90 nm across, 30 nm high, and discretized into 3 × 3 cubical cells. $\lambda = 543$ nm and the dielectric function is $\varepsilon = -6.65 + 1.98i$ for gold at this wavelength. Green's tensor's are evaluated in a plane 100 nm above the substrate.

elements opposed to one another across the diagonal of the matrix, the tensor clearly is not exactly antisymmetric. In the mixed tensors, extreme values strongly confined above the stadium boundary are found in the off-diagonal xy- and yx-components. The diagonal xx- and yy-components exhibit large contrasts around the four corners of the stadium with a point symmetry with respect to the center of the structure. In the zz-component there are multifold symmetry patterns around individual particles especially in the curved parts of the stadium. Also noticeable for G^{EE} and G^{HH}, the dominant feature of the remaining off-diagonal elements is the fact that the particles appear bright on one side and dark on the other. Maps of $G^{HE}(\mathbf{r},\mathbf{r})$ are very similar to $G^{EH}(\mathbf{r},\mathbf{r})$, although some typical patterns get interchanged between components. Whether it is possible to image the components of the magnetic and mixed Green's tensors including their phase or sign in a near-field optics experiment, at present remains an open question.

8 Conclusions

Using Green's dyadic technique, it has been shown how modelling in near-field optics can be extended to setups with electric and magnetic sources as well as materials having both dielectric and magnetic permeabilities. Electric, magnetic and mixed susceptibility tensors can be constructed from analytically known basic components. In fact, the dielectric and magnetic properties of a given material distribution can be included sequentially by applying the same building scheme for the tensors twice. It has also been demonstrated that the method for calculating field distributions based on the Lippmann-Schwinger equation can be generalized in a straight-forward manner to the case with permeabilities as well as sources of both electric and magnetic type.

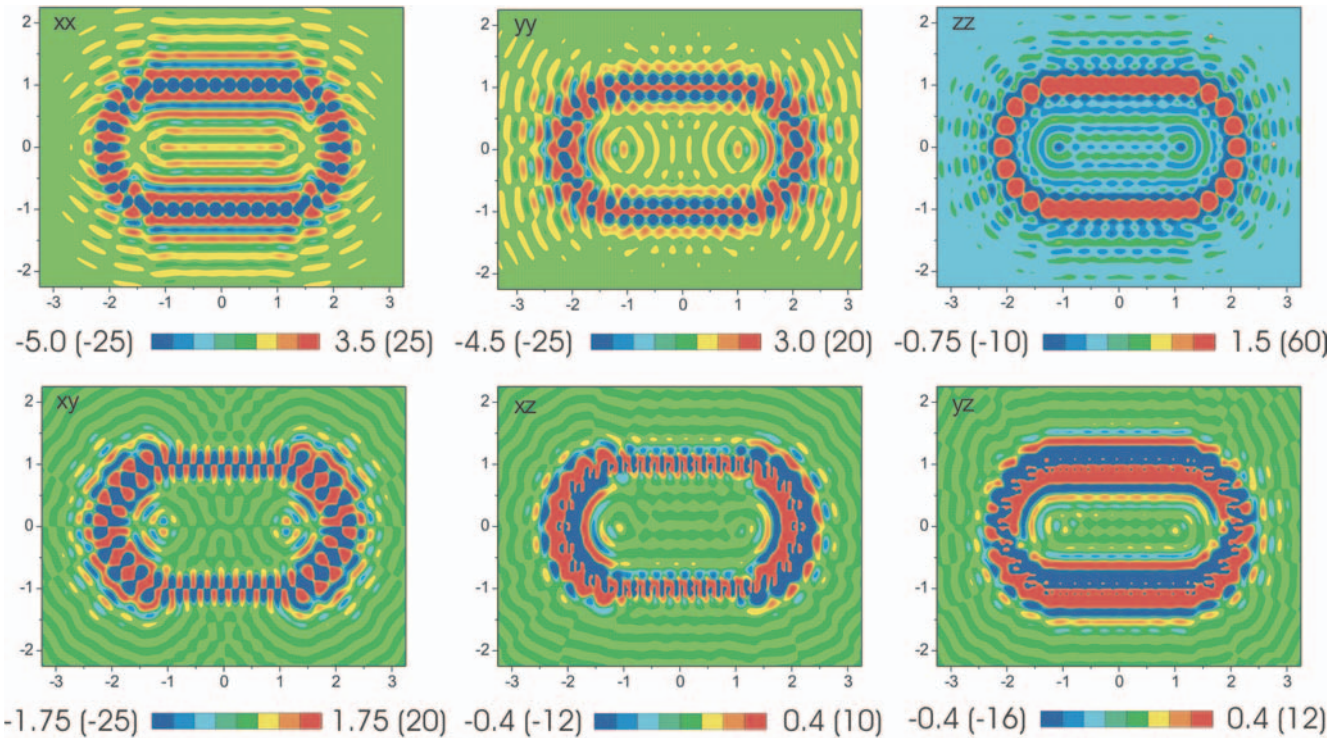

Fig. 8. Components of $-\mathrm{Im}G^{EE}(\mathbf{r},\mathbf{r})$ in a plane above the structure from Figure 7. Dimensions of the plot are in micrometers and the limits of the equidistant color scales are given; values beyond these limits are also plotted in blue or red resp. and the numbers in parenthesis are the minimum resp. maximum values from the calculation.

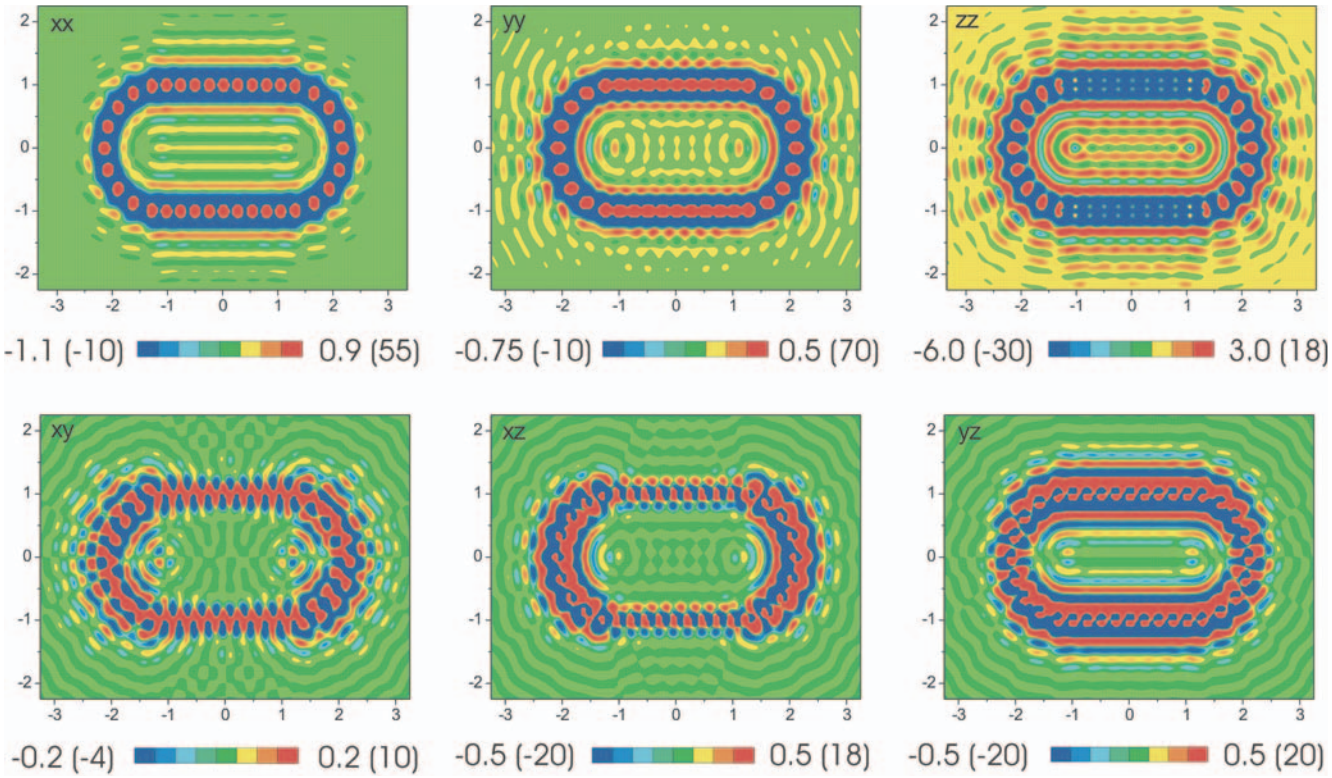

Fig. 9. Components of $-\mathrm{Im}G^{HH}(\mathbf{r},\mathbf{r})$.

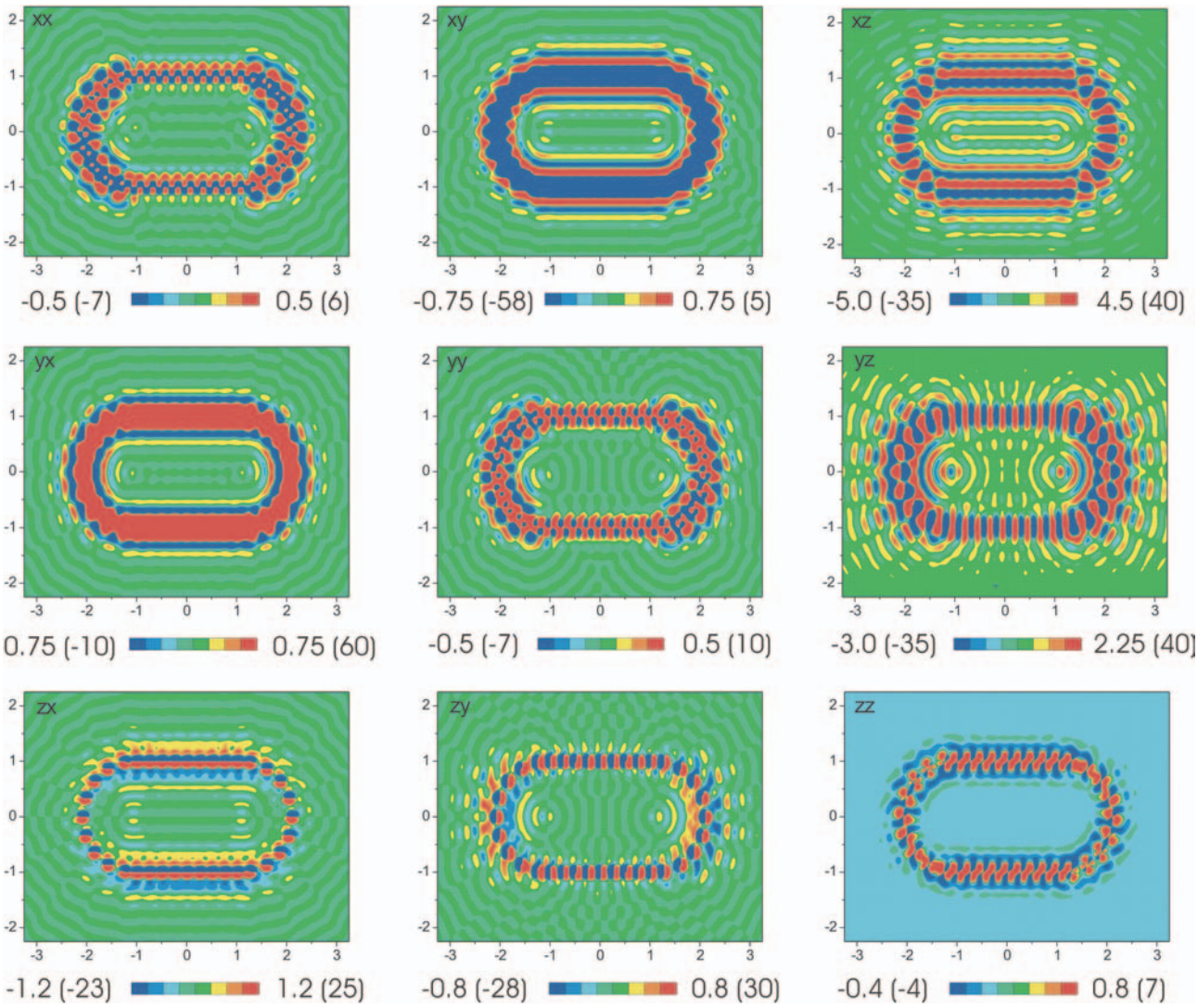

Fig. 10. Components of $\mathrm{Re}G^{EH}(\mathbf{r},\mathbf{r})$.

Finally, some example calculations for single pads as basic cases as well as on a coral structure currently of interest in near-field optics have been presented. Modelling of all field and susceptibility components will be of great help to interpret near-field optical images from both collecting and illuminating probe devices. As for metal cylinders with dielectric core [27] surface plasmons in holes in metal films as fabricated by Ebbesen and coworkers [33,34] can exhibit magnetic dipole moments comparable or even exceeding their electric dipole moments at optical frequencies. Such objects might thus become of interest as samples for near-field experiments. The type of tip used in [22,23] can sustain circular plasmon modes with considerable magnetic dipole moment and therefore maps the optical magnetic field in a passive probe device. A next important step would consist in using this kind of tip in an active probe NSOM device. In this way it could be possible to realize a magnetic dipole like point source and perhaps image the optical magnetic density of states in addition to the electric density of states [20].

Thanks to Alain Dereux, Jean-Claude Weeber and Christian Girard who introduced me to Green's dyadic technique and Cédric Chicanne and Eloise Devaux whose experimental work stimulated these theoretical investigations. I am also grateful to Elke Scheer for the freedom to work on this subject.

Appendix A: Comment on background with a surface

For completeness we would first like to note here that in the limit $\mathbf{r}' \to \mathbf{r}$ G^0 has to be replaced by [11]

$$G^0(\mathbf{r},\mathbf{r}) = -\frac{4\pi}{3} \times \mathbf{1} \tag{A.1}$$

and Q^0 is to be taken as

$$Q^0(\mathbf{r},\mathbf{r}) = 0. \tag{A.2}$$

With a surface, the background propagator is G_E^h for the electric and G_H^h for the magnetic field. If for the medium above the surface $\varepsilon_b = 1$ and $\mu_b = 1$, like G^0

$$
\begin{aligned}
&-\nabla\wedge\frac{1}{\varepsilon}\nabla\wedge G_\varepsilon^{HH}+k_0^2\,G_\varepsilon^{HH}=-\nabla\wedge\nabla\wedge G_\varepsilon^{HH}-\nabla\wedge\left(\frac{1}{\varepsilon}-1\right)\nabla\wedge G_\varepsilon^{HH}+k_0^2\,G_\varepsilon^{HH}\\
&=-\nabla\wedge\nabla\wedge G_H^h-\nabla\wedge\nabla\wedge k_0^2Q_{HE}^0V\left(\mathbf{1}-G_E^hV\right)^{-1}Q_{EH}^0-\nabla\wedge\left(\frac{1}{\varepsilon}-1\right)\nabla\wedge G_H^h\\
&\quad-\nabla\wedge\left(\frac{1}{\varepsilon}-1\right)\nabla\wedge k_0^2Q_{HE}^0V\left(\mathbf{1}-G_E^hV\right)^{-1}Q_{EH}^0+k_0^2G_H^h+k_0^4Q_{HE}^0\left(\mathbf{1}-G_E^hV\right)^{-1}Q_{EH}^0\\
&=-k_0^2G_H^h-4\pi k_0^2\mathbf{1}\delta\left(\mathbf{r}-\mathbf{r}'\right)-k_0^4Q_{HE}^0V\left(\mathbf{1}-G_E^hV\right)^{-1}Q_{EH}^0-4\pi k_0^2\nabla\wedge V\left(\mathbf{1}-G_E^hV\right)^{-1}Q_{EH}^0\\
&\quad-\nabla\wedge\left(\frac{1}{\varepsilon}-1\right)k_0^2Q_{EH}^0-\nabla\wedge\left(\frac{1}{\varepsilon}-1\right)k_0^2G_E^hV\left(\mathbf{1}-G_E^hV\right)^{-1}Q_{EH}^0\\
&\quad-\nabla\wedge\left(\frac{1}{\varepsilon}-1\right)4\pi k_0^2V\left(\mathbf{1}-G_E^hV\right)^{-1}Q_{EH}^0+k_0^2G_H^h+k_0^4Q_{HE}^0V\left(\mathbf{1}-G_E^hV\right)^{-1}Q_{EH}^0\\
&=-4\pi k_0^2\mathbf{1}\delta\left(\mathbf{r}-\mathbf{r}'\right)-4\pi k_0^2\nabla\wedge\frac{\varepsilon-1}{4\pi}\left(\mathbf{1}-G_E^hV\right)^{-1}Q_{EH}^0-\nabla\wedge\left(\frac{1}{\varepsilon}-1\right)k_0^2Q_{EH}^0\\
&\quad-\nabla\wedge\left(\frac{1}{\varepsilon}-1\right)k_0^2G_E^hV\left(\mathbf{1}-G_E^hV\right)^{-1}Q_{EH}^0-4\pi k_0^2\nabla\wedge\left(\frac{1}{\varepsilon}-1\right)\frac{\varepsilon-1}{4\pi}\left(\mathbf{1}-G_E^hV\right)^{-1}Q_{EH}^0\\
&=-4\pi k_0^2\mathbf{1}\delta\left(\mathbf{r}-\mathbf{r}'\right)-\nabla\wedge\left(\frac{1}{\varepsilon}-1\right)k_0^2Q_{EH}^0-\nabla\wedge\left(\frac{1}{\varepsilon}-1\right)k_0^2G_E^hV\left(\mathbf{1}-G_E^hV\right)^{-1}Q_{EH}^0\\
&\quad-\nabla\wedge\left(1-\frac{1}{\varepsilon}\right)k_0^2[\mathbf{1}+G_E^hV\left(\mathbf{1}-G_E^hV\right)^{-1}]Q_{EH}^0\\
&=-4\pi\;k_0^2\;\mathbf{1}\;\delta\left(\mathbf{r}-\mathbf{r}'\right).
\end{aligned}
$$

these tensors there satisfy

$$
\begin{aligned}
-\nabla_{\mathbf{r}}\;\wedge\;\nabla_{\mathbf{r}}\wedge G_E^h(\mathbf{r},\mathbf{r}')\;+\;k_0^2\;G_E^h(\mathbf{r},\mathbf{r}')&=\\
-\,4\pi\;k_0^2\;\mathbf{1}\;\delta(\mathbf{r}-\mathbf{r}')&\qquad(A.3)\\
-\nabla_{\mathbf{r}}\;\wedge\;\nabla_{\mathbf{r}}\wedge G_H^h(\mathbf{r},\mathbf{r}')\;+\;k_0^2\;G_H^h(\mathbf{r},\mathbf{r}')&=\\
-\,4\pi\;k_0^2\;\mathbf{1}\;\delta(\mathbf{r}-\mathbf{r}').&\qquad(A.4)
\end{aligned}
$$

(For background permeabilities other than 1, $k_0=\omega/c$ has to be changed into $k_0=\sqrt{\varepsilon_b\mu_b}\omega/c$ before evaluating analytic expressions like (2.9) for these tensors. Besides that G_E^h only gets an additional factor $1/\varepsilon_b$ and G_H^h a factor $1/\mu_b$.) Eventually even including the influence of the surface, call Q_{HE}^0 the tensor describing the magnetic field caused by an electric point dipole and Q_{EH}^0 the tensor giving the electric field due to a magnetic dipole. Between Q_{HE}^0, Q_{EH}^0, G_E^h and G_H^h we have the fundamental relations

$$
\begin{aligned}
&\nabla_{\mathbf{r}}\wedge G_E^h(\mathbf{r},\mathbf{r}')=k_0^2\;Q_{HE}^0(\mathbf{r},\mathbf{r}')&(A.5)\\
&\nabla_{\mathbf{r}}\wedge Q_{HE}^0(\mathbf{r},\mathbf{r}')=G_E^h(\mathbf{r},\mathbf{r}')\;+\;4\pi\;\mathbf{1}\;\delta(\mathbf{r}-\mathbf{r}')&(A.6)\\
&\nabla_{\mathbf{r}}\wedge\nabla_{\mathbf{r}}\;\wedge\;Q_{HE}^0(\mathbf{r},\mathbf{r}')\cdot\ldots=k_0^2\;Q_{HE}^0(\mathbf{r},\mathbf{r}')\cdot\ldots\\
&\qquad+\;4\pi\;\delta(\mathbf{r}-\mathbf{r}')\;\nabla_{\mathbf{r}'}\;\wedge\ldots&(A.7)\\
&\nabla_{\mathbf{r}}\wedge G_H^h(\mathbf{r},\mathbf{r}')=k_0^2\;Q_{EH}^0(\mathbf{r},\mathbf{r}')&(A.8)\\
&\nabla_{\mathbf{r}}\wedge Q_{EH}^0(\mathbf{r},\mathbf{r}')=G_H^h(\mathbf{r},\mathbf{r}')+4\pi\;\mathbf{1}\;\delta(\mathbf{r}-\mathbf{r}')&(A.9)\\
&\nabla_{\mathbf{r}}\wedge\nabla_{\mathbf{r}}\;\wedge\;Q_{EH}^0(\mathbf{r},\mathbf{r}')\cdot\ldots=k_0^2\;Q_{EH}^0(\mathbf{r},\mathbf{r}')\cdot\ldots\\
&\qquad+\;4\pi\;\delta(\mathbf{r}-\mathbf{r}')\;\nabla_{\mathbf{r}'}\;\wedge\ldots&(A.10)
\end{aligned}
$$

If it is just the free space propagators G^0 and Q^0, these relations follow from (2.9) and (2.25). Here (A.5) and (A.8) can be understood as definitions for Q_{HE}^0 and Q_{EH}^0. Then (A.6), (A.7), (A.9) and (A.10) follow from these together with (A.3) and (A.4). It is assumed here that the effect of the surface is calculated exactly, which is in principle possible [6,9,10,25,28,31]. However, for one dielectric surface, the situation typically encountered in near-field optics, the electrostatic approximation usually suffices for modelling. The approximated tensors no longer fully satisfy (A.3) and (A.6), but, of course, the relations (A.3)-(A.10) for the exact background tensors are the ones the proofs of the characteristic equations for the Green's tensors from (3.1)-(3.4) and (4.1)-(4.4) are based on.

Appendix B: Tensor equation for G_ϵ^{HH}

As an example here is the detailed proof that G_ε^{HH} from (3.4) solves (3.7). We use (A.3)-(A.10) and (2.20).

(*see equation above*)

All proofs of this type are written out in the supplementary file maths.ps. A numerical algorithm for calculating the Green's tensors is outlined in tensors.ps.

References

1. M. Kahl, E. Voges, Phys. Rev. B **61**, 14078 (2000)
2. J.P. Kottmann, O.J.F. Martin, D.R. Smith, S. Schultz, Chem. Phys. Lett. **341**, 1 (2001)
3. H. Xu, M. Käll, Phys. Rev. Lett. **89**, 246802 (2002)
4. C. Girard, A. Dereux, Rep. Prog. Phys. **59**, 657 (1996)

5. O.J.F. Martin, C. Girard, A. Dereux, Phys. Rev. Lett. **74**, 526 (1995)
6. A. Dereux, thesis, Namur 1991
7. W.C. Chew, *Waves and Fields in Inhomogeneous Media* (IEEE Press, 1995)
8. M. Paulus, O.J.F. Martin, Phys. Rev. E **63**, 066615 (2001)
9. M. Paulus, O.J.F. Martin, J. Opt. Soc. Am. A **18**, 854 (2001)
10. M. Paulus, P. Gay-Balmaz, O.J.F. Martin, Phys. Rev. E **62**, 5797 (2000)
11. O.J.F. Martin, N.B. Piller, Phys. Rev. E **58**, 3909 (1998)
12. J.-C. Weeber, C. Girard, J.R. Krenn, A. Dereux, J.-P. Goudonnet, J. Appl. Phys. **86**, 2576 (1999)
13. J.R. Krenn, J.-C. Weeber, A. Dereux, E. Bourillot, Y. Lacroute, J.-P. Goudonnet, G. Schider, W. Gotschy, A. Leitner, F.R. Aussenegg, C. Girard, Phys. Rev. B **60**, 5029 (1999)
14. C. Girard, A. Dereux, C. Joachim, Phys. Rev. E **59**, 6097 (1999)
15. J.-C. Weeber, A. Dereux, C. Girard, G. Colas des Francs, J.R. Krenn, J.-P. Goudonnet, Phys. Rev. E **62**, 7381 (2000)
16. R. Quidant, J.-C. Weeber, A. Dereux, D. Peyrade, G. Colas des Francs, C. Girard, Y. Chen, Phys. Rev. E **64**, 066607 (2001)
17. J.R. Krenn, A. Dereux, J.-C. Weeber, E. Bourillot, Y. Lacroute, J.-P. Goudonnet, G. Schider, W. Gotschy, A. Leitner, F.R. Aussenegg, C. Girard, Phys. Rev. Lett. **82**, 2590 (1999)
18. J.-C. Weeber, J.R. Krenn, A. Dereux, B. Lamprecht, Y. Lacroute, J.-P. Goudonnet, Phys. Rev. B **64**, 045411 (2001)
19. A. Dereux, C. Girard, J.-C. Weeber, J. Chem. Phys. **112**, 7775 (2000)
20. C. Chicanne, T. David, R. Quidant, J.-C. Weeber, Y. Lacroute, E. Bourillot, A. Dereux, G. Colas des Francs, C. Girard, Phys. Rev. Lett. **88**, 097402 (2002)
21. H.C. Manoharan, C.P. Lutz, D.M. Eigler, Nature **403**, 512 (2000)
22. E. Devaux, A. Dereux, E. Bourillot, J.-C. Weeber, Y. Lacroute, J.-P. Goudonnet, C. Girard, Appl. Surf. Sci. **164**, 124 (2000)
23. E. Devaux, A. Dereux, E. Bourillot, J.-C. Weeber, Y. Lacroute, J.-P. Goudonnet, C. Girard, Phys. Rev. B **62**, 10504 (2000)
24. A. Dereux, E. Devaux, J.-C. Weeber, J.-P. Goudonnet, C. Girard, J. Microscopy **202**, 320 (2001)
25. C. Girard, J.-C. Weeber, A. Dereux, O. Martin, J.-P. Goudonnet, Phys. Rev. B **55**, 16487 (1997)
26. J. Aizpurua, P. Hanarp, D.S. Sutherland, M. Käll, G.W. Bryant, F.J. Garcia de Abajo, Phys. Rev. Lett. **90**, 057401 (2003)
27. U. Schröter, A. Dereux, Phys. Rev. B **64**, 125420 (2001)
28. C. Girard, A. Dereux, O. J. F. Martin, M. Devel, Phys. Rev. B **52**, 2889 (1995)
29. E. Devaux, thesis, Dijon 2000
30. J.D. Jackson, *Classical Electrodynamics* (Wiley, 1975), Chap. 9.2
31. G.S. Agarwal, Phys. Rev. A **11**, 230 (1975)
32. G.C. desFrancs, C. Girard, J.-C. Weeber, C. Chicanne, T. David, A. Dereux, D. Peyrade, Phys. Rev. Lett. **86**, 4950 (2001)
33. T.W. Ebbesen, H.J. Lezec, H.F. Ghaemi, T. Thio, P.A. Wolff, Nature **391**, 667 (1998)
34. T. Thio, K.M. Pellerin, R.A. Linke, H.J. Lezec, T.W. Ebbesen, Opt. Lett. **26**, 1972 (2001)